Hindawi Publishing Corporation
Journal of Nanomaterials
Volume 2015, Article ID 567073, 15 pages
http://dx.doi.org/10.1155/2015/567073

Review Article

Review of Synthesis and Antioxidant Potential of Fullerenol Nanoparticles

Aleksandar Djordjevic,[1] Branislava Srdjenovic,[2] Mariana Seke,[3] Danijela Petrovic,[4] Rade Injac,[5] and Jasminka Mrdjanovic[6]

[1]*Department of Chemistry, Biochemistry and Environmental Protection, Faculty of Science, University of Novi Sad, Trg Dositeja Obradovica 3, 21000 Novi Sad, Serbia*
[2]*Department of Pharmacy, Medical Faculty, University of Novi Sad, Hajduk Veljkova 3, 21000 Novi Sad, Serbia*
[3]*Institute of Nuclear Sciences "Vinca", University of Belgrade, Vinca, Serbia*
[4]*Department of Natural Sciences and Mathematics, Faculty of Education Sombor, University of Novi Sad, 25000 Novi Sad, Serbia*
[5]*Institute of Pharmaceutical Biology, University of Ljubljana, Askerceva 7, 1000 Ljubljana, Slovenia*
[6]*Oncology Institute of Vojvodina, Faculty of Medicine, University of Novi Sad, Put Dr. Goldmana 4, 21204 Sremska Kamenica, Serbia*

Correspondence should be addressed to Aleksandar Djordjevic; aleksandar.djordjevic@dh.uns.ac.rs

Received 16 April 2015; Accepted 25 June 2015

Academic Editor: Soumen Das

This review describes the chemical synthesis of polar polyhydroxylated fullerene C_{60} derivatives, fullerenols $C_{60}(OH)_n$, $2 \le n \le 44$, $C_{60}H_zO_x(OH)_y$, and polyanion fullerenols $C_{60}(OH)_{15}(ONa)_9$, ranging from the very first synthetic methods up to some contemporary approaches to synthesis and separation. It also provides some basic information about physical characteristics of fullerenols. With the increasing number of hydroxyl groups, water solubility of fullerenols increases as well. Fullerenols both in water and biological media build nanoparticles of different dimensions and stability. In different chemical and biological model systems a large number of various polyhydroxylated fullerene derivatives were tested and they showed both their antioxidative and prooxidative characteristics. Several mechanisms have been proposed for the antioxidant activity of fullerenol. In addition, this paper also provides insight into patents referring to the antioxidant properties of fullerenol.

1. Introduction

Since its discovery by Kroto et al. in 1985, fullerene C_{60} molecule has had a significant impact on many scientific directions with a very interesting history [1]. Starting from fundamental research of cluster carbon structures all the way to industrial production, fullerenes and their derivatives have now found a place in commercial products. Fullerene C_{60}, unlike graphite and diamond, is chemically very reactive. So far, a large number of different chemical reactions and derivatives of fullerene C_{60} have been published in scientific papers [2, 3]. Spherical fullerene C_{60} behaves as an electron-deficient alkene and readily reacts with electron-rich species. Attachment of various polar functional groups or molecules on the fullerene core overcomes the almost complete insolubility of C_{60}, while retaining the unique inherent fullerene properties, and achieves reasonable biological availability [3–5]. Several synthetic paths of fullerenols with various degrees of fullerenes hydroxylation $C_{60}(OH)_n$, $2 \le n \le 44$, polyanion fullerenols $C_{60}(OH)_{15}(ONa)_9$, metallofullerenes $Gd@C_{82}(OH)_{22}$, and other fullerene derivatives have been published [6–20]. In aqueous solutions, depending on the pH value, fullerenols are more or less deprotonated and exist in the form of fullerenol nanoparticles (FNP). FNP are mostly important in the biological application of fullerenes, especially due to their antioxidant properties. Several mechanisms of FNP antioxidant activity are proposed here: the radical-addition reaction of $2n$ $OH^{\bullet}$ radicals to the remaining olefinic

double bonds of the fullerenol core, the ability of the hydroxyl radical to abstract hydrogen or an electron from fullerenol, and the formation of coordinative bonds with prooxidant metal ions. It has been shown in different model systems that FNP prevent the process of lipid peroxidation and possess superoxide, hydroxyl radical, and nitric oxide scavenging activity. The unique electronic π-system of fullerene C_{60} and its derivatives make them potential photosensitizers upon the absorption of UV or visible light.

2. Fullerene C_{60}

The fullerene C_{60} form of carbon was named after the American architect Buckminster Fuller, who was famous for designing a large geodesic dome which slightly resembles the molecular structure of C_{60}. Fullerene is a compound composed solely of an even number of carbon atoms which form a three-dimensional cage-like fused ring polycyclic system with 12 five-membered rings and the rest are six-membered rings. All fullerenes have an even number of carbons. Spherical fullerene C_{60}, known as buckyball, is the most representative member of the fullerene family with the shape of an icosahedron, containing 12 pentagons and 20 hexagons. Fullerene carbon atoms are considered to be equivalent, since C_{60} shows a single line at $\delta = 143$ ppm in its ^{13}C NMR spectrum. C_{60} behaves as a three-dimensional electron-deficient polyolefin. The pentagonal structures in C_{60} molecule contain single bonds, and the bridging bonds between pentagonal and hexagonal structures contain double bonds. All fullerenes which obey the so-called isolated pentagon rule are considered to be stable. Fullerene C_{60} is practically insoluble in water and other polar solvents and slightly soluble in toluene and benzene; however, it is soluble in 1,2-dichlorobenzene, dimethylnaphthalenes, and 1-chloronaphthalene. The chemical properties of fullerene C_{60} are based on the fact that the bonding has delocalized π molecular orbitals extending throughout the structure, and the carbon atoms are a mixture of sp^2 and sp^3 hybridized systems. Fullerene C_{60} is not "superaromatic" as it tends to avoid double bonds in the pentagonal rings, resulting in poor electron delocalization. As a result, C_{60} behave as an electron deficient alkenes and reacts readily with electron-rich species. The main types of chemical reactions of C_{60} are nucleophilic addition, pericyclic reactions, radical additions, oxidation, electrophilic addition, halogenations, and the formation of endohedral complexes $M@C_{60}$, where M usually refers to an atom of metal [2]. Figure 1 presents the main chemical reactions on fullerene C_{60}.

The principal reactions are electrophilic addition reactions and are therefore exothermic in most cases (these reactions are accompanied by a charge of hybridization of the carbon atoms from sp^2 to sp^3, which reduces angular strain in the cage). The number of addends decreases the exothermic heat of the reaction. Therefore, adducts with a high degree of addition become unstable. As a result, a great number of isomers are formed that is one of the biggest problems in the synthesis of only one derivative. For example, two addends $C_{60}X_2$ can have eight regioisomers (23 stereoisomers). The chemical properties of C_{60} (nucleophilic and electrophilic additions, pericyclic reactions, and radical additions) enable the covalent bonding of many different organic compounds and functional groups on its cage. Water-soluble fullerene-based derivatives are the most important for the biological application of fullerenes.

3. Water-Soluble Fullerene C_{60} Based Derivatives, Fullerenol $C_{60}(OH)_n$

The attachment of various polar functional groups or molecules to the fullerene core overcomes the almost complete insolubility of fullerene C_{60}, while it retains its unique inherent fullerene properties and achieves reasonable biological availability [3–5, 53, 54]. Fullerene derivatives have been widely investigated in various chemical and biological experimental models. Special attention has been paid to the investigation of carboxyfullerenes $C_{60}(CHCOOH)_{2-6}$, where the tris(dicarboxymethyl)-fullerene C3 isomer has been most extensively studied, as well as bisphosphonate fullerene derivatives and amino derivatives of fullerene $C_{60}(NH_2)_n$ [3–5].

Several synthesis paths of fullerenols with various degrees of hydroxylation and a general formula of $C_{60}(OH)_n$, $2 \leq n \leq 42$ or $C_{60}H_zO_x(OH)_y$ have been published since 1992. The solubility of a fullerene molecule is dependent on the number of introduced hydroxyl groups. The low-degree hydroxylated fullerenols $C_{60}(OH)_{10-12}$ can dissolve in some polar solvents, for example, THF, dimethylformamide (DMF), and dimethyl sulfoxide (DMSO), and the medium-degree fullerenols $C_{60}(OH)_{16}$ and $C_{60}(OH)_{20-24}$ are reported to dissolve even in water. The specific behavior of fullerenols is a consequence of their structural flexibility, the rotation of the OH groups around the axes going through the C–O bonds, and the distribution of these groups across different carbon sites of the fullerene surface [55]. Fullerenol in a molecular state can be obtained at concentrations below 20 mg/dm^3. The sonication of fullerenol solutions increased their agglomeration and caused the formation of nanofullerenol clusters predominately with diameters of 10.7 or 102 nm, suggesting that clusters of these sizes were more stable and, hence, energetically more favored, which was supported by zeta potential measurements [56]. The relationship between fullerenol concentration and zeta potential warrants a more in-depth sensitivity analysis in order to assess how higher concentrations impact biological response [6]. Fullerenols simultaneously have both attractive (C–OH) and repulsive (C–O–) sites. The acidic protons could be involved in attractive hydrogen bonding interactions with other fullerenol molecules, driving nanocluster formation which would decrease the hydrophobic portion of the molecular surface area [7]. Depending on the number of hydroxyl groups per C_{60} molecule, the pH values and concentration of fullerene stable nanoclusters range from 10 to 250 nm. Since the protonation state of polyhydroxylated C_{60} is pH dependent, in aqueous solutions, depending on the pH value, they are more or less deprotonated and exist in the form of stable polyanion nanoparticles. Most of the investigations of fullerene derivatives on biological model systems (especially investigations of antioxidant potential) were conducted with

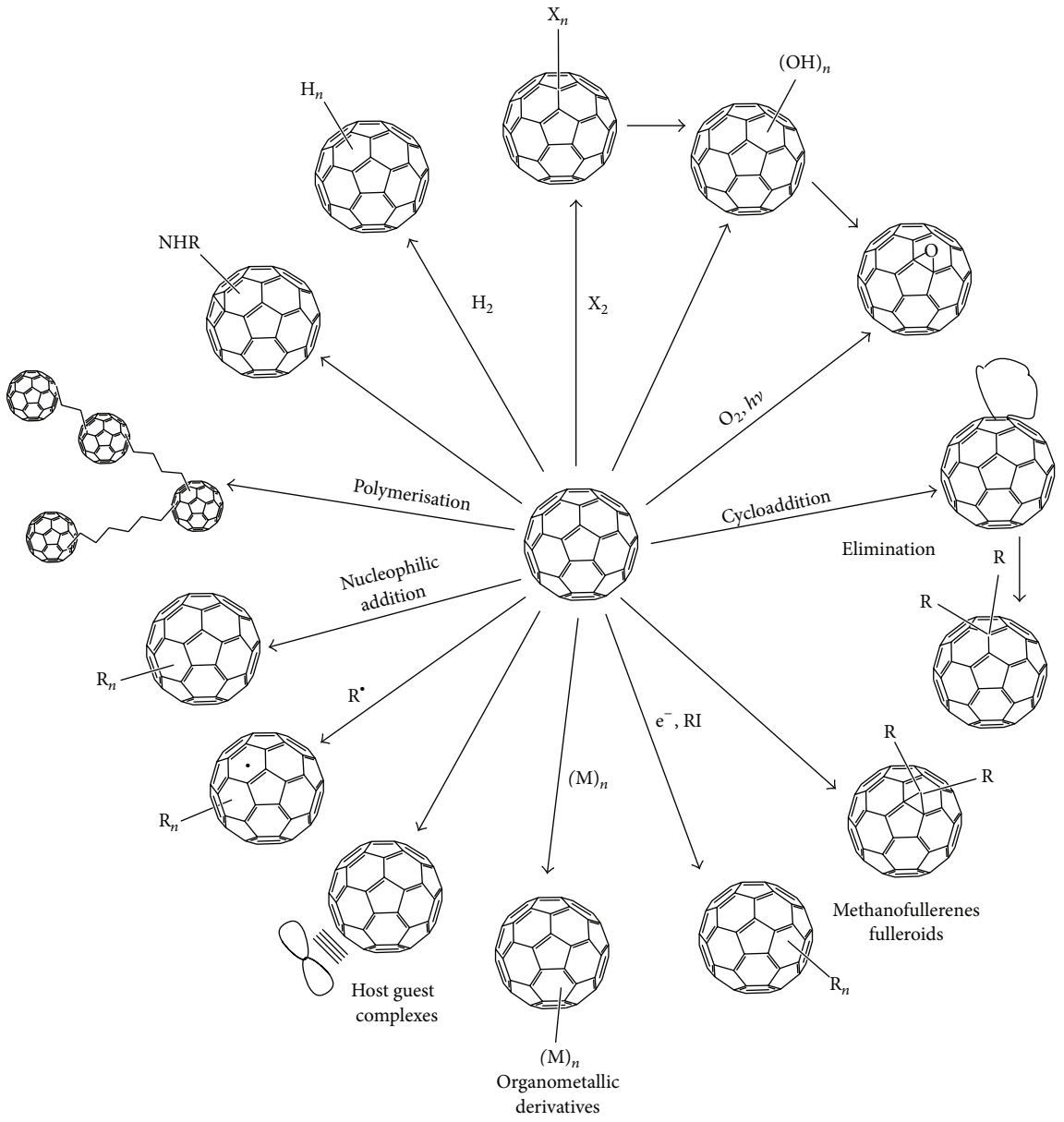

Figure 1: The chemical reactions on fullerene C_{60} [2].

the polyhydroxylated derivatives and endohedral fullerenes listed below:

$C_{60}(OH)_x$, $C_{60}(OH)_{10-12}$, $C_{60}(OH)_{16}$, $C_{60}(OH)_{20\pm2}$, $C_{60}(OH)_{22-24}$, $C_{60}(OH)_{24}$, $C_{60}(OH)_{36}$, $C_{60}(OH)_{44}$, $C_{60}H_zO_x(OH)_y$, $C_{60}O_5(OH)_{18}$, $C_{60}(OH)_{15}(ONa)_9$, $Gd@C_{82}(OH)_{22}$, $Na_n^+[C_{60}O_xOH_y]^{n-}$ (n = 2-3, x = 7–9, and y = 12–15).

3.1. Synthesis and Characterization of Hydroxylated Fullerene. Many methods for synthetizing polyhydroxylated fullerene C_{60} have been reported in scientific publications. Commercially available fullerenols (http://buckyusa.com/Polyhydroxy.htm) as well those synthetized in laboratory conditions have a certain variability in the chemical composition of the overall oxygen and monooxygenated surface groups. These products do not have good reproducibility in structural characterization which creates difficulties for experimental studies.

3.2. Polyhydroxylated Fullerene Derivatives $C_{60}(OH)_n$. In the early 1990s Li et al. synthesized C_{60} fullerenol with 24–26 hydroxyl groups directly by the reaction of fullerene C_{60} with aqueous NaOH in the presence of tetrabutylammonium hydroxide (TBAH), the most effective catalyst in aerobic conditions and at room temperature [8]. Methanol was used for the separation of the reaction mixture. IR spectra showed characteristic absorption bands at 3430 cm^{-1} (–OH), 1400, 1070 cm^{-1} (C–O), and 1600 cm^{-1} (C=C). In the ^1H NMR spectrum in DMSO-$d6$ the mean peak was found at δ =

3.35 ppm, while in D_2O *d*6 the mean peak was found at δ = 3.10 ppm. The ^{13}C NMR spectrum had one broad peak at δ = 140 ppm. Using elemental microanalysis Li et al. determined that synthesized fullerenol had 26,5 hydroxyl groups. The same procedure of fullerenol synthesis was done in an argon flow. The reaction was slower and a maximum 10 hydroxyl groups were attached to the fullerene core.

3.3. Fullerenol Synthetized Using Hemiketal Groups. In brief, a fullerene mixture of C_{60} (84%) and C_{70} (16%) was treated with oleum (H_2SO_4–SO_3), and the solution was stirred to give a green solution with suspension. An excess of potassium nitrate (KNO_3) was then added to this acid suspension at 5°C. The resulting aqueous acid solution was filtered through Celite under vacuum to remove insoluble particles. The filtrate was basified until the pH reached 9.0 or higher. During base neutralization, the color of the solution slowly turned dark with fine, brown suspensions. The precipitate was separated from the solution by a centrifuge technique and washed several times with a NaOH solution (1 mol/L) and methanol to provide brown solids of polyhydroxylated fullerene derivatives [9]. The spectral characteristics of the obtained fullerenol were as follows: IR = 3424 (–OH), 1595, 1392, 1084, and 593 cm^{-1}; ^{13}C NMR (D_2O) δ = 170.3, 140.3, 100.0, and 79.0 ppm; and solid-state ^{13}C NMR δ = 175.0, 141.1, 103.1, and 78.3 ppm. The basic analysis of the obtained fullerenol resulted in the following: C-43.5, H-3.1, O-46.9, N-0.52, Na-2.3, and S-1.6%. In the second method, the fullerenol was prepared as follows: a fullerene mixture of C_{60} (84%) and C_{70} was treated with concentrated sulfuric acid and concentrated nitric acid. The mixture was slowly heated to 115°C and stirred at that temperature for 4–6 h. It was cooled to room temperature and basified until the pH of the product solution reached 9.0 or higher. To provide brown solids of polyhydroxylated fullerene, the above explained separation procedure was carried out. The X-ray photoelectron spectroscopy analysis (XPS) indicated that obtained fullerenol molecule had monooxygenated carbons (287.9 eV, 23%) such as ethereal or hydroxylated carbons, dioxygenated carbons (289.7 eV, 9%) such as carbonyl (C=O), ketal (RO–C–OR), or hemiketal (RO–C–OH) carbons, and nonoxygenated carbons (286.1 eV, 68%). The estimation is that the average number of hydroxyl additions is 14–16 with approximately 6-7 hemiketal moieties per fullerene molecule. The solid-state ^{13}C NMR showed peaks at δ = 79.0 ppm (hydroxylated carbons), δ = 100.0 ppm (hemiketal carbons), δ = 140.3 ppm (unreacted olefinic carbons), and δ = 170.3 ppm (vinyl ether carbons). These spectra provided consistent evidence to support the structural assignment of fullerenols containing hemiketals with vinyl ether linkages. A TGA-mass spectroscopy analysis of fullerenol detected the thermal elimination of H_2O, CO from monooxygenated carbons and CO_2 from dioxygenated carbons.

3.4. Fullerenol Synthesis Using Hydroborate. An excess of the BH_3-THF complex was added to a solution of fullerene dissolved in dry toluene. The reaction mixture became increasingly brown due to precipitation of a solid intermediate, $C_{60}(HBH_2)_n$, leaving the supernatant toluene colorless [10]. The intermediate was then treated with a solution of H_2O_2 followed by NaOH. The resulting mixture was stirred for 3 h and allowed to settle overnight. The obtained brown precipitate was soluble in dimethyl sulfoxide and pyridine, sparingly soluble in diluted HCl and slightly soluble in water. The IR spectrum of the obtained precipitate was 3430, 1631, 1385, 1090, and 450–550 cm^{-1} (from unreacted fullerene). The above described procedure of fullerene derivatization in water-soluble form produces fullerenol with a variable number of hydroxyl and other functional groups. In the second procedure, a slight variation of reaction conditions was used for the synthesis of $C_{60}(HBH_2)_n$. The intermediate was than treated with glacial acetic acid and washed with $NaHCO_3$ solution. The IR spectrum of the residual solid in toluene gave characteristic IR stretching bands of C–H and O–H groups; ^1H NMR spectrum in C_6D_6 was found with a peak of δ = 5.88 ppm (C–H group) and two unidentified peaks at δ = 6.08 and 6.03 ppm.

3.5. Fullerenol Synthesis from Polybrominated Derivative. The procedure for catalytical bromination of C_{60} with elementary bromine with $FeBr_3$ as a catalyst is described in the paper published by Djordjević et al. In this procedure only one reaction product—$C_{60}Br_{24}$—was obtained without any occluded bromine molecules [57]. The excess of unreacted bromine was evaporated and the catalyst was separated from the reaction mixture by washing it with an acidic aqueous solution pH 2. A thermogravimetric analysis showed that in the process of thermal transformation all bromine atoms are lost, which is a characteristic of the completely symmetrical distribution of bromine over the C_{60} molecule. FTIR and ray analysis were in accordance with published data.

The polyhydroxylated polyanion C_{60} derivative, fullerenol $C_{60}(OH)_{24-n}O_n{}^-Na_n{}^+$, was obtained by complete substitution (SN2 mechanism) of bromine atoms from $C_{60}Br_{24}$ with hydroxyl groups in alkaline aqueous solution pH 12. The aqueous solution of fullerenol with residual amounts of NaOH and NaBr was applied on the top of the combined ion-exchange resin and eluted with demineralized water until discoloration. The solution of fullerenol (pH = 7) was evaporated under low pressure; a dark brown powder substance of fullerenol $C_{60}(OH)_{24}$ remained (see the following) [11].

Synthesis of fullerenol $C_{60}(OH)_{24}$ from polybrominated derivative $C_{60}Br_{24}$ [11] is as follows:

$$\begin{aligned} C_{60} + Br_2 &\xrightarrow[\substack{RT, t^0 \\ HCl}]{FeBr_3} C_{60}Br_{24} \\ &+ NaOH \xrightarrow[EtOH]{RT} C_{60}(OH)_{24-n}O_n{}^-Na_n{}^+ \\ &\xrightarrow{\text{ion exchange resin}} C_{60}(OH)_{24} \end{aligned} \quad (1)$$

Analysis: FTIR $C_{60}(OH)_{24}$: 3426 cm^{-1}, 1596 cm^{-1}, 1359 cm^{-1} 1062 cm^{-1}; ^1H NMR singlet peak at δ = 4.2 ppm; ^{13}C NMR peaks at δ = 107.0 ppm and δ = 158.8 ppm, UPLC retention time at 4.49 min MS/MS 1128 m/z; UV/VIS

maximum at 211 nm; TPD > 100°C (moisture), 252°C and 455°C. Water and DMSO as a cosolvent, physiological saline solution, cell culture media (DMEM, RPMI 1640), and human blood serum provide conditions for the good stability of fullerenol nanoparticles as is the case with water (or water/DMSO) and physiological saline.

The solubility of fullerenol in water was 11 mg/mL, while in the DMSO/water mixture (9 : 1 v/v) it was more than 37 mg/mL. The size distribution of particles by number analysis revealed the presence of particles of dimensions ranging from 10 to 50 nm, with a maximum of 15.7 nm. Fullerenol nanoparticles dissolved in water pH 6.5 had a negative charge $\zeta = -49.8$ mV. A change in the pH of the aqueous solution (from 2 to 11) affected the negative charge of the nanoparticles. Fullerenol nanoparticles are formed from the more organized molecules that can aggregate, and they form stable agglomerates ranging in dimension within 20–60 nm. AFM images of fullerenol nanoparticles in aqueous solution pH 6.5 are presented in Figure 2. AFM measurements of fullerenol nanoparticles are made by using the standard AFM tapping mode with a tip radius lower than 10 nm. Highly orientated pyrolytic graphite (HOPG) was used as a surface.

Structures of fullerenol molecule $C_{60}(OH)_{24}$ and fullerenol polyanion nanoparticles $C_{60}(OH)_{24-n}O_n^-Na_n^+$ are presented in Figure 3. The space between the polyanion molecules in nanoparticles is filled with water molecules connected with hydrogen bonds. The ability of $C_{60}(OH)_{24-n}O^-_nNa^+$ to self-assemble opens the possibility of the application of nanoparticles as a nanodelivery system of active principles in biological models.

3.6. Fullerenol Synthesis Using PEG 400 as a Catalyst. Zhang et al. synthesized fullerenols via the direct reaction of fullerene with aqueous NaOH comprising polyethylene glycol (PEG) 400 as a catalyst [12]. The substitution of TBAH with PEG 400 as a catalyst represents a modification of the method described by Li et al. [8]. Depending on the reaction conditions, either water-soluble C_{60} fullerenol (fullerenol 1) or water-insoluble C_{60} fullerenol (fullerenol 2) could be obtained selectively. The elemental analyses of fullerenols 1 and 2 showed an average composition of ($n = 8.5$ and 27 for 1 and 2, resp.). Both fullerenols showed similar IR spectra: 3432 cm^{-1}, 1063 cm^{-1}, and 1600 cm^{-1}; ^{1}H NMR spectra were also similar: a single strong peak centered at $\delta = 3.35$ ppm, corresponding to hydroxyl protons. With the increase of the concentration of PEG and NaOH, the conversion of fullerene to water insoluble fullerenol (fullerenol 2) was significantly accelerated. Longer reaction time was needed when the reaction was carried out in N_2 than in air, which proved that the PEG 400 was a more effective catalyst than some other catalysts such as TBAH. Addition of the aqueous NaOH to the benzene solution of C_{60} obtained a high percentage of water-soluble fullerenol 2.

3.7. Synthesis of Fullerenol Covered by More Than 18 Hydroxyl Groups. The starting material for the synthesis of fullerenol with more than 18 hydroxyl groups [13] was fullerenol 1 $C_{60}(OH)_{12}$, sodium free, synthesized by the method reported by Chiang et al. [14]. The starting material $C_{60}(OH)_{12}$ (fullerenol 1) was added to a 30% hydrogen peroxide solution, and the mixture was vigorously stirred for 4 days under air at 60°C until the suspension turned into a clear yellow solution. After the solution cooled down, the addition of a mixed solvent of 2-propanol, diethyl ether, and hexane gradually yielded a milky white precipitate. Drying of the residue gave 67% of pale yellow-brown powder of $C_{60}(OH)_{36}{\cdot}8H_2O$ (fullerenol 2). Similar treatment of $C_{60}(OH)_{12}$ (fullerenol 1) for a prolonged reaction time at 60°C for up to 2 weeks, within the same workup as given above, provided 68% of $C_{60}(OH)_{40}{\cdot}9H_2O$ (fullerenol 3) as a milky white powder. The IR spectra of fullerenols 2 and 3 were 3400, 1080, 1370, and 1620 cm^{-1}. The elemental analysis of fullerenol 2 resulted in $C_{60}(OH)_{36}{\cdot}8H_2O$ and fullerenol 3 resulted in $C_{60}(OH)_{40}{\cdot}9H_2O$. The solubility (25°C, pH 7) of fullerenol 2 was 17.5 mg/mL and fullerenol 3 58.9 mg/mL, while the solubility of polyanion fullerenol $C_{60}ONa_x(OH)_{16-x}$ was more than 200 mg/mL despite the moderate number of hydroxyl groups [15]. Such a type of water-soluble fullerenol might include a few sodium ions because of the synthetic process using NaOH as hydroxylation or neutralization reagent and the difficulty in complete removal of the sodium ion from the weakly acidic or chelation-natured fullerenol [7, 16]. Presumed mechanisms of fullerenol formation in an alkaline medium and by oxidation with molecular oxygen are shown in Figure 4 [16].

Because the simple acidification of fullerenol must induce the acid-catalyzed pinacol rearrangement, it is difficult to remove the sodium ion completely without using a column chromatography process. It is noteworthy that the water solubility of fullerenol 3 was much higher than that of 2 because of the greater number of hydroxyl groups of the former. The weight loss of fullerenol 2 ($C_{60}(OH)_{36}{\cdot}8H_2O$) was observed in three temperature ranges, that is, room temperature to 130°C, 130–350°C, and 350°C. The first weight loss is assigned to the secondary bound water; the second reduction might be attributed to dehydration of the introduced hydroxyl groups and, for example, by possible thermal pinacol rearrangement, whereas the third reduction might be attributed to the decomposition of the fullerene nucleus. The particle size of fullerenol 2 measured using dynamic light scattering (DLS) analysis was 1 nm. The addition of NaOH to the solution of fullerenol 2 up to pH 12 revealed a high extent of aggregation (50–100 nm) of the fullerenol, although the addition of HCl (pH 2.6) essentially did not affect the particle size. The observed phenomenon was rationalized on the basis of a strong interaction between the metal cation (Na^+) and the fullerenol, leading to aggregation or finally precipitation. Precipitation phenomena have not been noticed with alkali metals, while complete precipitation of fullerenol occurred with *alkaline earth metals* and *transition metals* [17]. Addition of a mixture of 2-propanol, diethyl ether, and hexane (5 : 5 : 5) into the reasonably concentrated aqueous solution of the fullerenol 2 or 3 led to the formation of fullerenol aggregation. The addition of the poor solvent probably reduced the solvation of the fullerenol by water molecules and increased the intermolecular hydrophobic interaction. The synthesis of $C_{60}(OH)_{36}{\cdot}8H_2O$ and $C_{60}(OH)_{40}{\cdot}9H_2O$ is presented in Figure 5.

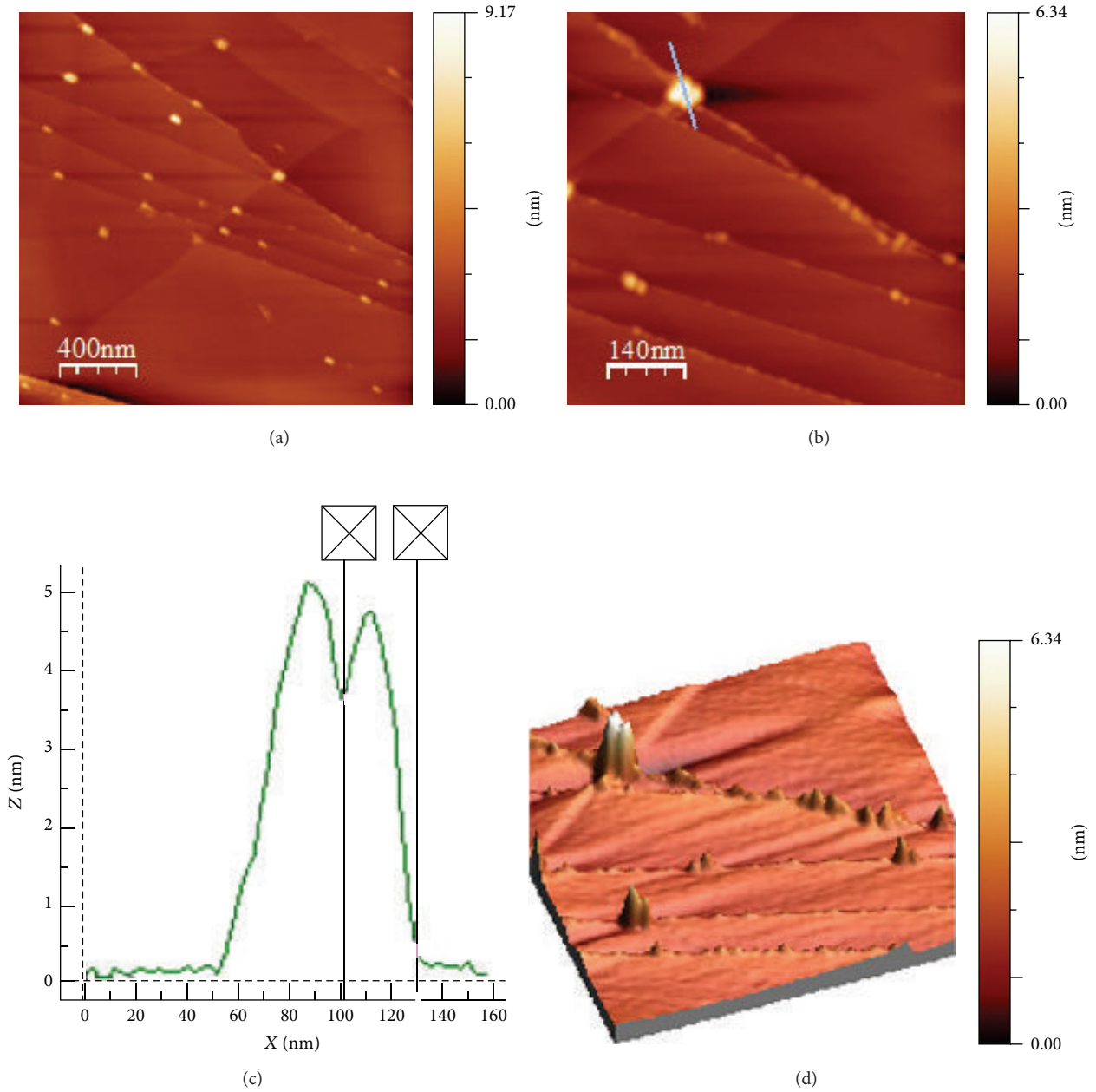

FIGURE 2: AFM images of fullerenol polyanion nanoparticles $C_{60}(OH)_{24-n}O_n^-Na_n^+$ in aqueous solution pH 6.5. (a) Large-scale image 2000 × 2000 nm^2, (b) small-scale image, 700 × 700 nm^2 of nanoparticles of about 100 nm on HOPG surface, and (c) corresponding cross-section of fullerenol nanoparticles. Maximal peak of the particle was 5.0 nm; smaller particle peak was 4.7 nm, respectively. (d) 3D image.

A possible reaction mechanism for the formation of the fullerenol with a high number of hydroxyl groups is that the basic hydroxide ion –OH induces hydroperoxide ion –OOH formation as a result of the slightly higher acidity of H_2O_2 than that of H_2O (Figure 6) [15, 18]. The formed –OOH attacks C_{60} to give fullerene epoxide $C_{60}O$, followed by the attack of –OH and protonation. The obtained fullerene epoxide was susceptible to subsequent nucleophilic attacks of –OH and –OOH because of the higher strain.

3.8. Synthesis of Fullerenol Prepared by the Direct Oxidation Route. Semenov et al. [19] started their synthesis of fullerenol by using fullerenol (fullerenol-d, i.e., fullerene-direct) synthesized by the method reported by Li et al. [8]. Briefly, a near-saturated solution of C_{60} in benzene was prepared and NaOH solution and solution of tetrabutylammonium hydroxide were added. Benzene was distilled and the resulting mixture was stirred for 12–15 h, during which time the resulting fullerenol-d was extracted to the aqueous phase. Adding methanol to the resulting solution caused the salting out of fullerenol-d from the aqueous solution as a brown flaky precipitate. The precipitate was separated from the liquid phase and additionally washed repeatedly with methanol until neutral pH 7 ± 1 was obtained, after which it was

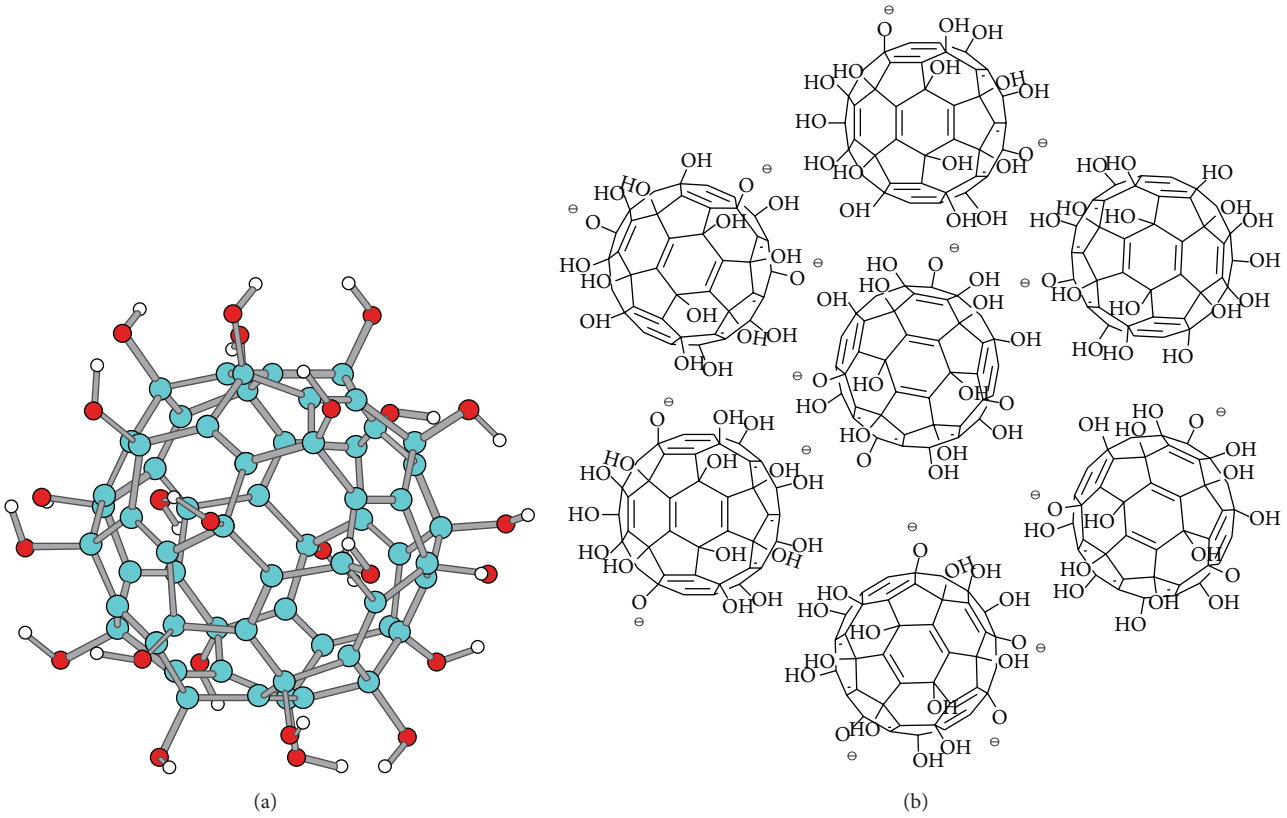

FIGURE 3: Structures of (a) the fullerenol molecule $C_{60}(OH)_{24}$ and (b) the fullerenol polyanion nanoparticles $C_{60}(OH)_{24-n}O_n{}^-Na_n{}^+$.

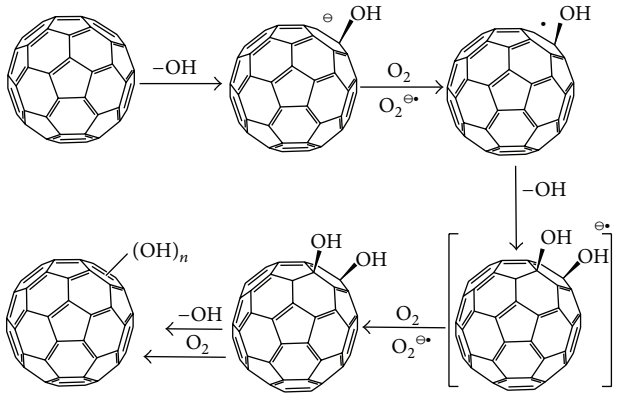

FIGURE 4: Presumed mechanisms of fullerenol formation in an alkaline medium and by oxidation with molecular oxygen [16].

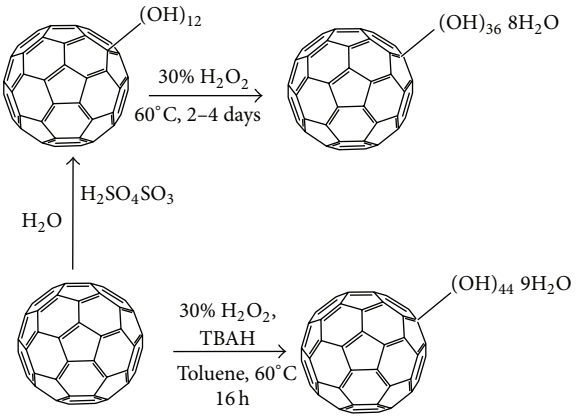

FIGURE 5: Synthesis of fullerenol $C_{60}(OH)_{36}{\cdot}8H_2O$ and $C_{60}(OH)_{40}{\cdot}9H_2O$ [13].

dried. The yield of red-brown crystals of fullerenol-d was 72%. FTIR spectra were 3420 cm^{-1}, 1590 cm^{-1}, 1450 cm^{-1}, and 1040 cm^{-1}; HPLC analysis determined the following: a broad peak maximum near 6.1 min. This indicates that the column that Semenov et al. employed did not allow the separation of the main product, fullerenol-d, since fullerenol-d is a mixture of polyalcohols $C_{60}(OH)_n$, oxypolyalcohols $C_{60}(OH)_{n1}O_{n2}$, or their salts $C_{60}(OH)_{n1}O_{n2}(ONa)_{n3}$. Qualitative mass spectra of fullerenol-d have distinctive peaks corresponding to $m/z \approx 970$–1317. The mean expectancies formula for fullerenol $m/z \approx 1094$–1128 was $C_{60}(OH)_{22-24}$.

3.9. Synthesis and Separation of Fullerenol Based on Dialysis. Fullerenol, prepared according to a two-phase reaction by using NaOH, contains Na ions [16]. A dialysis-based method was developed by Yao et al. to remove Na ions in fullerenol $C_{60}(OH)_{14-26}$ preparation [20]. The used dialysis membrane had a molecular weight cut-off (MWCO) of 8–15 kDa. A

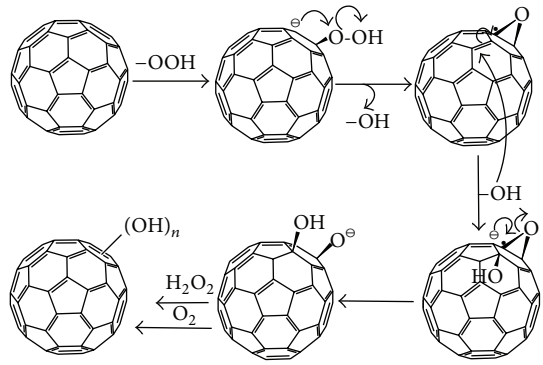

Figure 6: A possible reaction mechanism for the formation of fullerenol with a high number of hydroxyl groups with H_2O_2 [18].

dialysis route for fullerenol prepared by the reaction of fullerene with aqueous NaOH and tetrabutylammonium hydroxide (TBAH) is shown in Figure 7.

FTIR spectrum for purified fullerenol resulted in 1080 cm^{-1}, 1380 cm^{-1}, 1600 cm^{-1}, and 3400 cm^{-1}; ^1H NMR spectrum $\delta = 4.8$ ppm. More Na elements are eliminated by the prolonged dialysis time.

3.10. Synthesis of Fullerenol as a Single Nanoparticle. Kokubo et al. synthesized fullerenol $C_{60}(OH)_{44}$ in a facile one-step reaction from the toluene solution of C_{60} by hydroxylation with hydrogen peroxide in the presence of a phase-transfer catalyst, tetra-n-butylammonium hydroxide (TBAH) [18]. The mixture was stirred under air at 60°C until the purple toluene layer turned into a colorless transparent solution. An aqueous solution was separated and a mixed solvent of 2-propanol, diethyl ether, and hexane (7 : 5 : 5) was added to yield a milky white precipitate. The residual solid was washed with diethyl ether and dried. A pale yellow powder of fullerenol was obtained. To remove residual TBAH, fullerenol was dissolved in deionized water and the resulting yellow solution was passed through an active magnesium silicate. Addition of a mixed solvent afforded a brownish-yellow precipitate. The solid was washed with diethyl ether. Drying of the solid gave purified fullerenol 2 (67%) as a milky white to yellow powder. The IR spectrum of fullerenol 2 was 3400, 1080, 1370, and 1620 cm^{-1}. Weight losses for fullerenol 2 were observed in three temperature ranges on the TGA trace recorded: room temperature to 120°C, 120–250°C, and >250°C. The first weight loss can be assigned to secondary bound water; the second reduction can be attributed to the dehydration of the introduced hydroxyl groups, while the weight loss at the highest temperature (>250°C) can be attributed to the decomposition of the fullerene nucleus. The average structure of fullerenol 2 was deduced to be $C_{60}(OH)_{44}{\cdot}8H_2O$ from elemental analysis. Fullerenol 2 exhibited high water solubility, up to 64.9 mg/mL, under neutral (pH = 7) conditions. The narrow distribution of the particle sizes by number (1.46 ± 0.38 nm) indicates that fullerenol 2 is highly dispersed at a molecular level and that the usual aggregation of fullerenols is not prevalent. This could be because fullerenol 2 is surrounded by solvent-water molecules as a result of the strong hydrogen bonding with the introduced hydroxyl groups. The particle size distribution obtained from the induced grating method (IG method) was consistent with the previously mentioned DLS results. The average particle size was determined to be 0.806 nm ± 0.022 nm. To compare and verify the data obtained by the DLS and IG methods, Kokubo et al. conducted the particle size measurement again by means of scanning probe microscopy (SPM). The average particle size of fullerenol 2 was determined to be 1.03 nm ± 0.28 nm. The results of the particle size measurement by three different methods confirm that the highly hydroxylated fullerenol nanoparticles have a highly dispersed nature in water. The surface nanostructure of fullerenol 2 in powder form was also observed by SPM. It revealed nanoscale spherical structures of about 30–50 nm in diameter which combine with a second particle to form a larger third particle on a microscale. The solid state of fullerenol therefore exists in an aggregated form but disperses at a molecular level once it is dissolved in water. Table 1 shows the methods of synthesis of hydroxylated derivatives of C_{60}, fullerenols.

4. Antioxidative and Prooxidative Potential of Fullerenols

4.1. Scavenging Potential of Various Free Radical Types of Polyhydroxylated Derivatives of Fullerene. Many of the water-soluble fullerene derivatives have been recognized for their antioxidant properties: amphiphilic monoadducts of fullerene C_{60} [58], C3 and D3—trismalonyl C_{60} derivative [59], endohedral fullerenol $Gd@C_{82}(OH)_{22}$, and fullerenol $C_{60}(OH)_{22}$ [60–62]. Several mechanisms for the antioxidant activity of fullerenol nanoparticles (FNP) have been proposed. In aqueous solution, nanomolecules of fullerenol form hydrogen bonds with H_2O and other molecules of fullerenol, creating stable negatively charged nanoparticles. Electron spin resonance (ESR) spectroscopy revealed that fullerenol has the ability of the dose-dependent inhibition of the ESR signal intensity of DPPH (2,2-diphenyl-1-picrylhydrazyl) radical. The possible mechanism of the antioxidative activity of fullerenol $C_{60}(OH)_{24}$ is the radical-addition reaction of $2n$ $OH^{\bullet}$ radicals to the remaining olefinic double bonds of the fullerenol core to yield $C_{60}(OH)_{24} + 2n$ $OH^{\bullet}$ (n = 1–12), in a dose-dependentmanner. The other proposed mechanism is the possibility of a hydroxyl radical to abstract a hydrogen from fullerenol, including the formation of a relatively stable fullerenol radical $C_{60}(OH)_{23}O^{\bullet}$ [63]. In addition, a hydroxyl radical may abstract one electron from fullerenol yielding the radical cation $C_{60}(OH)_{24}{}^{+}$. One more proposed mechanism is that the polyanion nanoparticles have numerous free electron pairs from oxygen, distributed around the FNP, and have a great capacity to form coordinative bonds with prooxidant metal ions [17]. In a liposome model system of cell membranes, Mirkov et al. showed that FNP prevents the process of lipid peroxidation. Treatment of liposomes with $FeSO_4$ and ascorbic acid led to the oxidation of polyunsaturated fatty acid in liposomes and formation of TBARS. The results showed that fullerenol-induced dose-dependent inhibition of $FeSO_4$/ascorbic acid-stimulated formation of

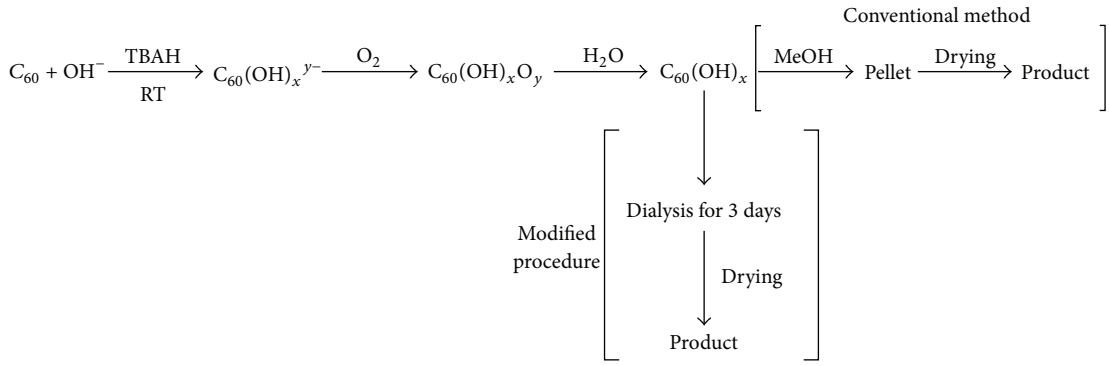

Figure 7: A dialysis route for fullerenol preparation [20].

Table 1: Methods of synthesis of hydroxylated derivatives of C_{60}, fullerenols.

Fullerenol	Methods	Characteristics	Ref.
$C_{60}(OH)_{24–26}$	Aqueous NaOH, TBAH, and O_2, 23°C	3430, 1400, 1070, and 1600 cm^{-1}; δ = 3.35 ppm, δ = 140 ppm	[8]
$C_{60}(OH)_nO_m$	C_{60}/C_{70} mix, H_2SO_4-SO_3, KNO_3, 5°C, pH ≥ 9, MeOH	3424, 1595, 1392, 1084, and 593 cm^{-1}; δ = 170.3, 140.3, 100.0, and 79.0 ppm, solid-state δ = 175.0, 141.1, 103.1, and 78.3 ppm	[9]
$C_{60}(OH)_nX$	BH_3-THF, H_2O_2, and NaOH	3430, 1631, 1385, 1090, and 450–550 cm^{-1}; δ = 5.88, 6.08, and 6.03 ppm	[10]
$C_{60}(OH)_{24}$	$Br_2/FeBr_3$, NaOH, and EtOH, 23°C	3426, 1596, 1359, and 1062 cm^{-1}, δ = 4.2 ppm; δ = 107.0, 158.8 ppm, t = 4.49 min, 211 nm, 252°C and 455°C, 10–50 nm, −49.8 mV	[11]
$C_{60}(OH)_n$	Aqueous NaOH, PEG 400	3432, 1063, and 1600 cm^{-1}, δ = 3.35 ppm	[12]
$C_{60}(OH)_{36}\cdot 8H_2O$ $C_{60}(OH)_{40}\cdot 9H_2O$	H_2O_2, 60°C, mix 2-propanol, diethyl ether, and hexane	3400, 1080, 1370, and 1620 cm^{-1}, 130–350°C, 50–100 nm	[13]
$C_{60}(OH)_{44}\cdot 8H_2O$	H_2O_2, mix 2-propanol, and diethyl ether	3400, 1080, 1370, and 1620 cm^{-1}, 23–120°C, 120–250°C, >250°C, 1.46 ± 0.38 nm	[18]
$C_{60}(OH)_{n1}O_{n2}(ONa)_{n3}$ $C_{60}(OH)_{22–24}$	Benzene, aqueous NaOH	3420, 1590, 1450, and 1040 cm^{-1}, 6.1 min, m/z 1094–1128	[19]
$C_{60}(OH)_{14–26}$	Aqueous NaOH, TBAH, and MWCO of 8–15 kDa	1080, 1380, 1600, and 3400 cm^{-1}, δ = 4.8 ppm	[20]

TBARS. In parallel, the authors examined the effect of butylated hydroxytoluene (BHT) on lipid peroxidation and the obtained results demonstrated that fullerenol possesses similar efficiency in the prevention of lipid peroxidation as BHT. For the determination of the superoxide radical scavenging activity of FNP, the authors applied fullerenol into the xanthine/xanthine oxidase system which caused a decrease in the reduction rate of cytochrome c compared to the control. The obtained result demonstrated that fullerenol in the range of nanomolar and micromolar concentrations decreased the reduction of cytochrome c between 5 and 20%, while concentration of 1 mM decreased reduction of cytochrome c for 40% [11]. The hypothetical mechanism of action of the polyanion fullerenol $C_{60}(OH)_{24}$ with the superoxide anion radical is presented in Figure 8 [52].

The antioxidant ability of the water-soluble derivative of fullerene $C_{60}(OH)_{32}\cdot 8H_2O$ was assessed by DMPO-spin trap/ESR method. This C_{60} derivative had an ability to diminish the ESR spectrum attributed to hydroxyl radicals. Meanwhile, a singlet radical-signal different from OH-attributed signals increased in a manner dependent on the concentrations of $C_{60}(OH)_{32}\cdot 8H_2O$. These results suggest that $C_{60}(OH)_{32}\cdot 8H_2O$ scavenges $OH^{\bullet}$ owing to the dehydrogenation of $C_{60}(OH)_{32}\cdot 8H_2O$ and is simultaneously oxidized to a stable fullerenol radical [64]. The antioxidant ability of $C_{60}(OH)_{32}\cdot 8H_2O$ was also confirmed in beta-carotene bleaching assay [65].

The first proof of the nitric oxide scavenging activity of FNP in different model systems was in the solution of SNP which is a spontaneous liberator of NO in the presence of light irradiation. The obtained results showed that the presence of fullerenol in a SNP solution decreased the levels of nitrite, in comparison to the nitrite levels obtained when SNP was dissolved alone. To test the possible *in vivo* NO-scavenging activity of FNP, the antioxidant defense in adult rat testis was used as a model system. The effects of the

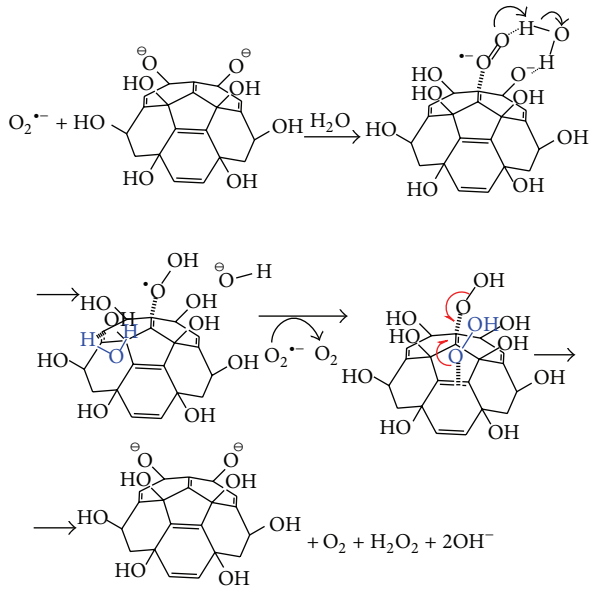

Figure 8: The hypothetical mechanism of action of the polyanion fullerenol $C_{60}(OH)_{24}$ with superoxide anion radical [52].

NO-scavenging activity of FNP on the activities of testicular antioxidant enzymes were investigated after intratesticular (i.t.) injection of SNP and fullerenol into each testis. Pretreatment of the rats with an i.t. injection of fullerenol completely prevented an SNP-induced reduction in the activities of catalase, glutathione *S*-transferase, and glutathione peroxidase. FNP, applied alone, did not induce any changes in the activity of the studied antioxidant enzymes, with the exception of decreased glutathione transferase activity. These results suggest that FNP possess NO-scavenging activity *in vivo* [11]. The scavenger activity of fullerenol with a smaller or moderate number of hydroxyl groups with OH radicals can be explained by addition to sp^2 carbon atoms [63, 66]. Table 2 presents the results of fullerenol scavenger activities in different biological systems.

4.2. Phototoxic Properties of Water-Soluble Fullerene Derivatives. The unique electronic π-system of fullerenes and its derivatives makes them potential photosensitizers upon the absorption of UV or visible light. Fullerenol $C_{60}(OH)_{24}$ produces a mixture of reactive oxygen species (ROS) under both visible and ultraviolet irradiation through two types of photochemical mechanisms [67], with the greatest rates of oxygen consumption at acidic pH (pH = 5) (see the following).

Potential reaction mechanisms of ROS generation via photosensitization of fullerenol $C_{60}(OH)_{24}$ [67] are as follows:

$$\begin{aligned} C_{60}(OH)_{24} &\longrightarrow C_{60}(OH)_{24}^{\bullet} \\ C_{60}(OH)_{24}^{\bullet} + O_2 &\longrightarrow C_{60}(OH)_{24} + {}^1O_2 \\ C_{60}(OH)_{24} + e^- (aq) &\longrightarrow C_{60}(OH)_{24}^{-\bullet} \\ C_{60}(OH)_{24}^{-\bullet} + O_2 &\longrightarrow C_{60}(OH)_{24} + O_2^{-\bullet} \end{aligned} \quad (2)$$

Evidence of both singlet oxygen ($^1O_2$) and superoxide production ($O_2^{-\bullet}$) was obtained and when compared to other known sensitizers of reactive oxygen, fullerenol $C_{60}(OH)_{24}$ produced more ROS at a rate at least two times that of other sensitizers. Because of all these features, fullerenol and other water-soluble derivatives could exhibit high toxicity toward epithelial cells and promote photocatalytic degradation of environmental hazards.

The formation of superoxide anion radical was observed when a solution of fullerenol $C_{60}(OH)_{24}$ was irradiated (>400 nm). Comparing phototoxicity toward HaCaT of (γ-CyD)$_2$/C_{60} (*c*-cyclodextrin bicapped C_{60}) and fullerenol, Zhao et al. concluded that fullerenol was less phototoxic [68]. The aggregation of fullerenol in aqueous solution results in a loss of its intrinsic photochemical reactivity with respect to the production of superoxide and singlet oxygen [69, 70]. The free radical (type I) mechanisms are considered to be involved in fullerenol phototoxicity.

4.3. Structures and Stabilities of Fullerenols. Antioxidative characteristics of the polyhydroxylated fullerene derivatives depend both on the number of hydroxyl groups and their arrangement on the C_{60} sphere [55, 67, 71]. Semiempirical calculations suggest that, in terms of thermodynamics, fullerenols are the most stable with 6 and 12 hydroxyl groups which are symmetrically arranged on the sphere of the C_{60} and with the smallest number of double bonds, 5, 6 [14, 72, 73]. Another method, such as density functional theory, suggests that the structures with 7 hydroxyl groups arranged on the one side of the C_{60} sphere are the most stable. The next stable structure is the one with 14 hydroxyl groups symmetrically arranged on both sides of the C_{60} [74, 75]. Theoretically speaking, the fullerenol forms with 24 hydroxyl groups which are arranged on the equator of the C_{60} sphere are the most stable [76]. Fullerenols with more than 24 hydroxyl groups have a tendency to open and destabilize cages. Characteristic functional groups that may appear in an open cage include hydroxyls, epoxies, carbonyls, and hemiacetals [75]. Pitek et al. used theoretical models to show that a small cluster of fullerenol $C_{60}(OH)_{24}$ with 7 molecules is the most stable [56]. Fullerenols with about 20 hydroxyl groups form negatively charged nanoagglomerates in a wide pH range in water media and in the presence of cosolvents such as DMSO [7, 51].

4.4. Patents Related to the Antioxidant Properties of Fullerenol. The patents related to the antioxidant properties of fullerenol are listed in Table 3.

5. Conclusion

The paper presents the syntheses, stability, and main antioxidant characteristics of the fullerenol molecule on biological models. The largest number of fullerenol synthesis procedures was performed in acidic and alkaline conditions. The process of synthesis over a polybrominated precursor results in a reaction product with 24 hydroxyl groups on C_{60}. With an increase in the number of hydroxyl groups, the

Table 2: Fullerenol scavenger activities in different biological systems.

Fullerenol	Cells/animals	Main biological effects	Ref.
Fullerenol-1	Rat pheochromocytoma cell (PC12) lines	Neuroprotective antioxidant, inhibiting neuronal apoptosis	[21]
$C_{60}(OH)_{22–26}$	Human lens epithelial cells	Human lens epithelial cells, increasing ROS, apoptosis (phototoxicity)	[22]
$C_{60}(OH)_n$	L929 fibrosarcoma, C6 glioma, and U251 glioma	ROS-independent apoptosis	[23]
$C_{60}(OH)_{15}(ONa)_9$	Porcine renal proximal tubule cells	Mitochondrial dysfunction, cytoskeleton disruption, ↓ ATP, and autophagy	[24]
$C_{60}(OH)_{24}$	Human umbilical vein endothelial cells	Autophagy, ↓ cell growth	[25]
$C_{60}(OH)_{24}$	Human umbilical vein endothelial cells	G1 cell cycle block, ↑ Ca^{2+}, ↑ ICAM-1, tissue factor, and PS	[26]
$C_{60}(OH)_{24}$	Human HaCaT keratinocytes	Increasing $O_2^{-\bullet}$, ↓ mitochondrial activity	[27]
$C_{60}(OH)_{24}$	RAW 264.7 macrophages	Foam cell-like formation, ↑ LDL receptor expression, and ↑ MMP-9 secretion	[28]
$C_{60}(OH)_{18}$	Liver microsomes	UV significant lipids and proteins oxidative damage, generating ROS on photoexcitation	[29]
$C_{60}(OH)_{32}$	Human epidermal keratinocytes	Cell death, ↑ IL-8	[30]
$C_{60}(OH)_{22–26}$	Human lens epithelial	Sunlight to early cataractogenesis	[22]
$C_{60}(OH)_{22–26}$	Human retinal pigment epithelial cells	Light-produced superoxide, retinal phototoxic damage	[31]
$C_{60}(OH)_{24}$	Chinese hamster ovary cells (CHO-K1)	Strong antioxidant, influencing the cellular redox state	[32]
$C_{60}(OH)_{24}$	Human lung carcinoma A549 cells	Nrf2 upregulated expression of phase II antioxidant enzymes, p38 MAPK in Nrf2/HO-1 activation, attenuating oxidative stress-induced apoptosis	[33]
$C_{60}(OH)_{20}$	Breast cancer –metastasis (EMT-6)	Antitumor and antimetastatic activities, modulation of oxidative stress in tumor tissues	[34]
$C_{60}(OH)_{24}$	Human leukemic cells (K562)	Overexpression Bcl-2 and Bcl-xL, GSTA4, MnSOD, NOS, CAT, and HO-1 genes	[35]
$C_{60}(OH)_{6–12}$, $C_{60}(OH)_{32–34}\cdot 7H_2O$, $C_{60}(OH)_{44}\cdot 8H_2O$	Human skin keratinocytes HaCaT	Radical-scavenging effects and cytoprotective effects, hydroxyl-radical scavenging activities, UVA or UVB irradiation-induced injuries, and intracellular reactive oxygen species-scavenging	[36]
$C_{60}(OH)_{24}$	Human neuroblastoma cells	Protecting cells from MPP^+ induced decreases, expression of nuclear factor-E2-related factor 2, expression and activity of γ-glutamyl cysteine ligase, level of glutathione, and mitochondrial protective antioxidant	[37]
$C_{60}(OH)_{n>36}$	Nematodes, *Caenorhabditis elegans*	Antioxidative stress, upregulating of several antistress genes, DAF-16, and aakg-4	[38]
$C_{60}(OH)_{18–22}(OK_4)$	Brain zebrafish, *Danio rerio*	↑ AChE expression, antioxidant behavior, and GCLC and GCLR expression	[39]
$C_{60}(OH)_{24}$	Fathead minnow (*Pimephales promelas*)	Suppressed neutrophil function, inhibitors of cytochrome P450-dependent monooxygenases	[40]
$C_{60}(OH)_{22–24}$	Intratracheal instillation (rat)	Bronchitis/alveolitis, ↑ neutrophil counts, and cellular damage markers in the BAL fluid	[41]
$C_{60}(OH)_{20\pm2}$	Intratracheal instillation (mouse)	Neutrophil inflammatory response, ↑ MCP-1 in the BAL fluid at 10 mg/kg	[42]
$C_{60}O_5(OH)_{18}$	Intraperitoneal injection (mouse)	LD_{50} = 1200 mg/kg, weight loss, and ↓ cytochrome P-450-dependent monooxygenase activity in the liver	[43]
Fullerenol-1	Rat adrenal gland, pheochromocytoma	Neuroprotective antioxidant, inhibiting neuronal apoptosis	[21]
$C_{60}(OH)_x$, $x = 22, 24$	Sprague-Dawley rats	Hepatotoxicity and nephrotoxicity, antioxidant ability	[44]
$C_{60}(OH)_{24}$	Sprague-Dawley rats, liver	Antioxidant protecting hepatocytes against doxorubicin toxicity and irritability of the peritoneum and abdominal tissue	[45]

Table 2: Continued.

Fullerenol	Cells/animals	Main biological effects	Ref.
$C_{60}(OH)_{24}$	Sprague-Dawley outbred rats	Doxorubicin inhibition of lung oxidative stress	[46]
$C_{60}(OH)_{24}$	Sprague-Dawley outbred rats	Preventing oxidative stress, lipid peroxidation, and the disbalance of GSH/GSSG, potential nephroprotector	[47]
$C_{60}(OH)_{24}$	Wistar male rat with colorectal cancer	Antioxidant protecting against doxorubicin-induced chronic cardio- and hepatotoxicity	[48]
$C_{60}(OH)_{24}$	Wistar rats	Antioxidant protecting doxorubicin-induced oxidative stress in the hemoglobin and the erythrocytes	[49]
$C_{60}(OH)_{2}$	Male Wistar rats	Antioxidant protecting doxorubicin-induced nephro-, testicular, and pulmonary toxicity	[50]
$C_{60}(OH)_{24}$	Wistar rat uteri (virgo intacta)	Reducing the level of GR increased in the presence of DMSO and modulates the activity of GR; cryopreservation to maintain the GSH level in medium	[51]
$C_{60}(OH)_{24}$	Wistar rats, testis	Direct scavenging activity of nitric oxide radical (NO), superoxide anion ($O_2^{-\bullet}$)	[11]

Table 3: List of patents related to the antioxidant properties of fullerenol.

Authors and name of patent	Patent number
Li Hui; Chen Shou; Wang Chunru; and Ju Xuecheng: Chitosan-Fullerol Compound, Preparation Method Thereof Compound and Moisture-Preserving Antioxidant	CN103156784 (A) 2013-06-19
Li Hui, Chen Shou; and Wang Chunru: Equipment for Producing Fullerol	CN103086344 (A)
Jiang Lung-Yung, Liu Feng-Jou, Li Yuan-De, Lai Yi-Lung, Tsai Ming-Jeng: Water-Soluble Fullerenol Pharmaceutical Composition	TW516958 (B) 2003-01-11
Yujie Xu, Min Liu, Baixia Yang, Junjie Sun Xu Yujie, Liu, Min, Yang Baixia, and Sun Junjie: Fullerenol Solid Lipid Nano-Particles, Preparation Method Thereof, and Application Thereof	CN102488657 (A)
Zhao Yuliang Chen and Yuliang Chen Zhao: Application of Metal Fullerol in Inhibiting Tumor Growth	CN1739562 (A)
Zhang Yazhou Tang and Yazhou Tang Zhang: Method for Synthesizing Gadolinium Metal Fullerol Using Ultrasonic Wave	CN1743264 (A)
Zhao Yuliang Chen [Cn], Yuliang Chen Zhao, Xing, Gengmei, Chen Chunying, and Zhao Yuliang: Metal Fullerol and Its Pharmaceutical Use for Inhibiting Tumor Growth	CN1935812 (A)
Ruili Liu, Xiaoqing CaI, Wenxin Li, Liu Ruili, Cai Xiaoqing, and Li Wenxin: Application of Fullerol in Beauty Treatment Skin Care Products	CN101239026 (A)
K. E. Geckeler and Yulan Wang: Preparation of Fullerenol Having Nanolayer or Nanowire Structures	US2005/0098776 A1, 12.5.
Krushna Vijay, Moungil Brij, and Koopman Ben: Systems and Methods Based on Radiation Induced Heating or Ignition of Functionalized Fullerenes	WO 2008/140576 A2
Kozeev Evgenij Aleksandrovich: Method of Producing Fullerenol C_{84} from Carbon Nanocluster Sulpho-Adduct Production Wastes	RU2496773 (C1)
Chunru Wang, Qu Chen, Li Jiang, Wang Chunru, Chen Qu, and Jiang Li: Method for Preparing High Water Solubility Fullerol	CN102583303 (A)
Long Y. Chinag: Fullerene Derivatives as Free Radical Scavengers	US 5648523

water solubility of fullerenols increases as well. Fullerenols with a larger number of hydroxyl groups were derived by alkaline procedure synthesis. With the increasing number of hydroxyl groups per C_{60} sphere, the number of other potential functional groups, such as carbonyls and epoxies, increases likewise. Defining the fullerenol structure in such cases is more complex. Thermodynamically, the most stable fullerenol structure is the one with 24 hydroxyl groups, which is theoretically described with the OH groups arranged on the C_{60} sphere. The experimentally proven structure with 24 hydroxyl groups is characterized by the symmetrically arranged distribution of the OH groups on the C_{60} cage. Fullerenols with up to 26 hydroxyl groups tend to form agglomerates of nanometric sizes in aqueous solutions. Fullerenols have shown excellent antioxidant characteristics in many biological models. In certain photoinduction cases fullerenols show prooxidative characteristics. The scavenging activity of the *polyanion* fullerenols with 24 hydroxyl groups with O_2 is explained through the formation of the peroxyradicals on fullerenol. The greatest number of biological studies has been conducted with fullerenols $C_{60}(OH)_{20–26}$. The characteristic of these fullerenols (with the mean number of

hydroxyl groups) to form stable polyanion nanoagglomerates both in water and other biological media indicates a possible basic path of antioxidative characteristics in biological models.

Conflict of Interests

The authors declare that there is no conflict of interests regarding the publication of this paper.

Acknowledgment

This study was supported by a grant from the Ministry of Education, Science and Technological Development of the Republic of Serbia, Grant no. III 45005.

References

[1] H. W. Kroto, J. R. Heath, S. C. O'Brien, R. F. Curl, and R. E. Smalley, "C_{60}: buckminsterfullerene," *Nature*, vol. 318, no. 6042, pp. 162–163, 1985.

[2] A. Hirsch and M. Brettreich, "Cluster modified fullerenes," in *Fullerenes*, pp. 345–358, Wiley, 2005.

[3] F. Cataldo and T. Da Ros, *Medicinal Chemistry and Pharmacological Potential of Fullerenes and Carbon Nanotubes*, Springer, 2008.

[4] A. Djordjevic, G. Bogdanovic, and S. Dobric, "Fullerenes in biomedicine," *Journal of the Balkan Union of Oncology*, vol. 11, no. 4, pp. 391–404, 2006.

[5] J. Grebowski, P. Kazmierska, and A. Krokosz, "Fullerenols as a new therapeutic approach in nanomedicine," *BioMed Research International*, vol. 2013, Article ID 751913, 9 pages, 2013.

[6] S. Assemi, S. Tadjiki, B. C. Donose, A. V. Nguyen, and J. D. Miller, "Aggregation of fullerol $C_{60}(OH)_{24}$ nanoparticles as revealed using flow field-flow fractionation and atomic force microscopy," *Langmuir*, vol. 26, no. 20, pp. 16063–16070, 2010.

[7] B. Vileno, P. R. Marcoux, M. Lekka, A. Sienkiewicz, T. Fehér, and L. Forró, "Spectroscopic and photophysical properties of a highly derivatized C_{60} fullerol," *Advanced Functional Materials*, vol. 16, no. 1, pp. 120–128, 2006.

[8] J. Li, A. Takeuchi, M. Ozawa, X. Li, K. Saigo, and K. Kitazawa, "C_{60} fullerol formation catalysed by quaternary ammonium hydroxides," *Journal of the Chemical Society, Chemical Communications*, no. 23, pp. 1784–1785, 1993.

[9] L. Y. Chiang, R. B. Upasani, J. W. Swirczewski, and S. Soled, "Evidence of hemiketals incorporated in the structure of fullerols derived from aqueous acid chemistry," *Journal of the American Chemical Society*, vol. 115, no. 13, pp. 5453–5457, 1993.

[10] N. S. Schneider, A. D. Darwish, H. W. Kroto, R. Taylor, and D. R. M. Walton, "Formation of fullerols via hydroboration of fullerene-C_{60}," *Journal of the Chemical Society, Chemical Communications*, no. 4, pp. 463–464, 1994.

[11] S. M. Mirkov, A. N. Djordjevic, N. L. Andric et al., "Nitric oxide-scavenging activity of polyhydroxylated fullerenol, $C_{60}(OH)_{24}$," *Nitric Oxide: Biology and Chemistry*, vol. 11, no. 2, pp. 201–207, 2004.

[12] J.-M. Zhang, W. Yang, P. He, and S.-Z. Zhu, "Efficient and convenient preparation of water-soluble fullerenol," *Chinese Journal of Chemistry*, vol. 22, no. 9, pp. 1008–1011, 2004.

[13] K. Kokubo, K. Matsubayashi, H. Tategaki, H. Takada, and T. Oshima, "Facile synthesis of highly water-soluble fullerenes more than half-covered by hydroxyl groups," *ACS Nano*, vol. 2, no. 2, pp. 327–333, 2008.

[14] L. Y. Chiang, L.-Y. Wang, J. W. Swirczewski, S. Soled, and S. Cameron, "Efficient synthesis of polyhydroxylated fullerene derivatives via hydrolysis of polycyclosulfated precursors," *The Journal of Organic Chemistry*, vol. 59, no. 14, pp. 3960–3968, 1994.

[15] S. Wang, P. He, J.-M. Zhang, H. Jiang, and S.-Z. Zhu, "Novel and efficient synthesis of water-soluble [60]fullerenol by solvent-free reaction," *Synthetic Communications*, vol. 35, no. 13, pp. 1803–1808, 2005.

[16] L. O. Husebo, B. Sitharaman, K. Furukawa, T. Kato, and L. J. Wilson, "Fullerenols revisited as stable radical anions," *Journal of the American Chemical Society*, vol. 126, no. 38, pp. 12055–12064, 2004.

[17] R. Anderson and A. R. Barron, "Reaction of hydroxyfullerene with metal salts: a route to remediation and immobilization," *Journal of the American Chemical Society*, vol. 127, no. 30, pp. 10458–10459, 2005.

[18] K. Kokubo, S. Shirakawa, N. Kobayashi, H. Aoshima, and T. Oshima, "Facile and scalable synthesis of a highly hydroxylated water-soluble fullerenol as a single nanoparticle," *Nano Research*, vol. 4, no. 2, pp. 204–215, 2011.

[19] K. N. Semenov, D. G. Letenko, N. A. Charykov et al., "Synthesis and identification of fullerenol prepared by the direct oxidation route," *Russian Journal of Applied Chemistry*, vol. 83, no. 12, pp. 2076–2080, 2010.

[20] L. Yao, F. Kang, Q. Peng, and X. Yang, "An improved method for fullerol preparation based on dialysis," *Chinese Journal of Chemical Engineering*, vol. 18, no. 5, pp. 876–879, 2010.

[21] H.-M. Huang, H.-C. Ou, S.-J. Hsieh, and L.-Y. Chiang, "Blockage of amyloid beta peptide-induced cytosolic free calcium by fullerenol-1, carboxylate C_{60} in PC_{12} cells," *Life Sciences*, vol. 66, no. 16, pp. 1525–1533, 2000.

[22] J. E. Roberts, A. R. Wielgus, W. K. Boyes, U. Andley, and C. F. Chignell, "Phototoxicity and cytotoxicity of fullerol in human lens epithelial cells," *Toxicology and Applied Pharmacology*, vol. 228, no. 1, pp. 49–58, 2008.

[23] A. Isakovic, Z. Markovic, B. Todorovic-Marcovic et al., "Distinct cytotoxic mechanisms of pristine versus hydroxylated fullerene," *Toxicological Sciences*, vol. 91, no. 1, pp. 173–183, 2006.

[24] D. N. Johnson-Lyles, K. Peifley, S. Lockett et al., "Fullerenol cytotoxicity in kidney cells is associated with cytoskeleton disruption, autophagic vacuole accumulation, and mitochondrial dysfunction," *Toxicology and Applied Pharmacology*, vol. 248, no. 3, pp. 249–258, 2010.

[25] H. Yamawaki and N. Iwai, "Cytotoxicity of water-soluble fullerene in vascular endothelial cells," *American Journal of Physiology—Cell Physiology*, vol. 290, no. 6, pp. C1495–C1502, 2006.

[26] M. P. Gelderman, O. Simakova, J. D. Clogston et al., "Adverse effects of fullerenes on endothelial cells: fullerenol $C_{60}(OH)_{24}$ induced tissue factor and ICAM-I membrane expression and apoptosis in vitro," *International Journal of Nanomedicine*, vol. 3, no. 1, pp. 59–68, 2008.

[27] B. Zhao, Y.-Y. He, P. J. Bilski, and C. F. Chignell, "Pristine (C_{60}) and hydroxylated [$C_{60}(OH)_{24}$] fullerene phototoxicity towards HaCaT keratinocytes: type I vs type II mechanisms," *Chemical Research in Toxicology*, vol. 21, no. 5, pp. 1056–1063, 2008.

[28] Y. Niwa and N. Iwai, "Nanomaterials induce oxidized low-density lipoprotein cellular uptake in macrophages and platelet aggregation," *Circulation Journal*, vol. 71, no. 3, pp. 437–444, 2007.

[29] J. P. Kamat, T. P. A. Devasagayam, K. I. Priyadarsini, and H. Mohan, "Reactive oxygen species mediated membrane damage induced by fullerene derivatives and its possible biological implications," *Toxicology*, vol. 155, no. 1–3, pp. 55–61, 2000.

[30] J. G. Saathoff, A. O. Inman, X. R. Xia, J. E. Riviere, and N. A. Monteiro-Riviere, "In vitro toxicity assessment of three hydroxylated fullerenes in human skin cells," *Toxicology in Vitro*, vol. 25, no. 8, pp. 2105–2112, 2011.

[31] A. R. Wielgus, B. Zhao, C. F. Chignell, D.-N. Hu, and J. E. Roberts, "Phototoxicity and cytotoxicity of fullerol in human retinal pigment epithelial cells," *Toxicology and Applied Pharmacology*, vol. 242, no. 1, pp. 79–90, 2010.

[32] B. Srdjenovic, M. Slavić, K. Stankov et al., "Size distribution of fullerenol nanoparticles in cell culture medium and their influence on antioxidative enzymes in Chinese hamster ovary cells," *Hemijska Industrija*, p. 54, 2015.

[33] S. Ye, M. Chen, Y. Jiang et al., "Polyhydroxylated fullerene attenuates oxidative stress-induced apoptosis via a fortifying Nrf2-regulated cellular antioxidant defence system," *International Journal of Nanomedicine*, vol. 9, no. 1, pp. 2073–2087, 2014.

[34] F. Jiao, Y. Liu, Y. Qu et al., "Studies on anti-tumor and antimetastatic activities of fullerenol in a mouse breast cancer model," *Carbon*, vol. 48, no. 8, pp. 2231–2243, 2010.

[35] K. Stankov, I. Borisev, V. Kojic, L. Rutonjski, G. Bogdanovic, and A. Djordjevic, "Modification of antioxidative and antiapoptotic genes expression in irradiated K562 cells upon fullerenol $C_{60}(OH)_{24}$ nanoparticle treatment," *Journal of Nanoscience and Nanotechnology*, vol. 13, no. 1, pp. 105–113, 2013.

[36] Y. Saitoh, A. Miyanishi, H. Mizuno et al., "Super-highly hydroxylated fullerene derivative protects human keratinocytes from UV-induced cell injuries together with the decreases in intracellular ROS generation and DNA damages," *Journal of Photochemistry and Photobiology B: Biology*, vol. 102, no. 1, pp. 69–76, 2011.

[37] X. Cai, H. Jia, Z. Liu et al., "Polyhydroxylated fullerene derivative $C_{60}(OH)_{24}$ prevents mitochondrial dysfunction and oxidative damage in an MPP^+-induced cellular model of Parkinson's disease," *Journal of Neuroscience Research*, vol. 86, no. 16, pp. 3622–3634, 2008.

[38] W. Cong, P. Wang, Y. Qu et al., "Evaluation of the influence of fullerenol on aging and stress resistance using *Caenorhabditis elegans*," *Biomaterials*, vol. 42, pp. 78–86, 2015.

[39] A. M. da Rocha, J. R. Ferreira, D. M. Barros et al., "Gene expression and biochemical responses in brain of zebrafish Danio rerio exposed to organic nanomaterials: carbon nanotubes (SWCNT) and fullerenol ($C_{60}(OH)_{18-22}(OK_4)$)," *Comparative Biochemistry and Physiology A: Molecular and Integrative Physiology*, vol. 165, no. 4, pp. 460–467, 2013.

[40] B. Jovanović, L. Anastasova, E. W. Rowe, and D. Palić, "Hydroxylated fullerenes inhibit neutrophil function in fathead minnow (Pimephales promelas Rafinesque, 1820)," *Aquatic Toxicology*, vol. 101, no. 2, pp. 474–482, 2011.

[41] A. Xu, Y. Chai, T. Nohmi, and T. K. Hei, "Genotoxic responses to titanium dioxide nanoparticles and fullerene in gpt delta transgenic MEF cells," *Particle and Fibre Toxicology*, vol. 6, article 3, 2009.

[42] M. Roursgaard, S. S. Poulsen, C. L. Kepley, M. Hammer, G. D. Nielsen, and S. T. Larsen, "Polyhydroxylated C_{60} fullerene (fullerenol) attenuates neutrophilic lung inflammation in mice," *Basic and Clinical Pharmacology and Toxicology*, vol. 103, no. 4, pp. 386–388, 2008.

[43] T.-H. Ueng, J.-J. Kang, H.-W. Wang, Y.-W. Cheng, and L. Y. Chiang, "Suppression of microsomal cytochrome P450-dependent monooxygenases and mitochondrial oxidative phosphorylation by fullerenol, a polyhydroxylated fullerene C_{60}," *Toxicology Letters*, vol. 93, no. 1, pp. 29–37, 1997.

[44] J.-Y. Xu, Y.-Y. Su, J.-S. Cheng et al., "Protective effects of fullerenol on carbon tetrachloride-induced acute hepatotoxicity and nephrotoxicity in rats," *Carbon*, vol. 48, no. 5, pp. 1388–1396, 2010.

[45] R. Injac, M. Perse, N. Obermajer et al., "Potential hepatoprotective effects of fullerenol $C_{60}(OH)_{24}$ in doxorubicin-induced hepatotoxicity in rats with mammary carcinomas," *Biomaterials*, vol. 29, no. 24-25, pp. 3451–3460, 2008.

[46] R. Injac, N. Radic, B. Govedarica et al., "Acute doxorubicin pulmotoxicity in rats with malignant neoplasm is effectively treated with fullerenol $C_{60}(OH)_{24}$ through inhibition of oxidative stress," *Pharmacological Reports*, vol. 61, no. 2, pp. 335–342, 2009.

[47] R. Injac, M. Boskovic, M. Perse et al., "Acute doxorubicin nephrotoxicity in rats with malignant neoplasm can be successfully treated with fullerenol $C_{60}(OH)_{24}$ *via* suppression of oxidative stress," *Pharmacological Reports*, vol. 60, no. 5, pp. 742–746, 2008.

[48] R. Injac, M. Perse, M. Cerne et al., "Protective effects of fullerenol $C_{60}(OH)_{24}$ against doxorubicin-induced cardiotoxicity and hepatotoxicity in rats with colorectal cancer," *Biomaterials*, vol. 30, no. 6, pp. 1184–1196, 2009.

[49] V. D. Milic, K. Stankov, R. Injac et al., "Activity of antioxidative enzymes in erythrocytes after a single dose administration of doxorubicin in rats pretreated with fullerenol $C_{60}(OH)_{24}$," *Toxicology Mechanisms and Methods*, vol. 19, no. 1, pp. 24–28, 2009.

[50] B. Srdjenovic, V. Milic-Torres, N. Grujic, K. Stankov, A. Djordjevic, and V. Vasovic, "Antioxidant properties of fullerenol $C_{60}(OH)_{24}$ in rat kidneys, testes, and lungs treated with doxorubicin," *Toxicology Mechanisms and Methods*, vol. 20, no. 6, pp. 298–305, 2010.

[51] M. Slavic, A. Djordjevic, R. Radojicic et al., "Fullerenol $C_{60}(OH)_{24}$ nanoparticles decrease relaxing effects of dimethyl sulfoxide on rat uterus spontaneous contraction," *Journal of Nanoparticle Research*, vol. 15, no. 5, article 1650, 2013.

[52] A. Dordević and G. Bogdanović, "Fullerenol: a new nanopharmaceutic?" *Archive of Oncology*, vol. 16, no. 3-4, pp. 42–45, 2008.

[53] A. Djordjevic, R. Injac, D. Jovic, J. Mrdjanovic, and M. Seke, "Bioimpact of carbon nanomaterials," in *Advanced Carbon Materials and Technology*, pp. 193–271, John Wiley & Sons, 2014.

[54] I. Rade, R. Natasa, G. Biljana, D. Aleksandar, and S. Borut, "Bioapplication and activity of fullerenol $C_{60}(OH)_{24}$," *African Journal of Biotechnology*, vol. 7, no. 25, pp. 4940–4950, 2008.

[55] E. E. Fileti, R. Rivelino, F. de Brito Mota, and T. Malaspina, "Effects of hydroxyl group distribution on the reactivity, stability and optical properties of fullerenols," *Nanotechnology*, vol. 19, no. 36, Article ID 365703, 2008.

[56] A. Pitek, A. Dawid, and Z. Gburski, "The properties of small fullerenol cluster $(C_{60}(OH)_{24})_7$: computer simulation," *Spectrochimica Acta Part A: Molecular and Biomolecular Spectroscopy*, vol. 79, no. 4, pp. 819–823, 2011.

[57] A. Djordjević, M. Vojinović-Miloradov, N. Petranović, A. Devečerski, D. Lazar, and B. Ribar, "Catalytic preparation and

characterization of $C_{60}Br_{24}$," *Fullerene Science and Technology*, vol. 6, no. 4, pp. 689–694, 1998.

[58] P. Witte, F. Beuerle, U. Hartnagel et al., "Water solubility, antioxidant activity and cytochrome C binding of four families of exohedral adducts of C_{60} and C_{70}," *Organic & Biomolecular Chemistry*, vol. 5, no. 22, pp. 3599–3613, 2007.

[59] A. A. Corona-Morales, A. Castell, A. Escobar, R. Drucker-Colín, and L. Zhang, "Fullerene C_{60} and ascorbic acid protect cultured chromaffin cells against levodopa toxicity," *Journal of Neuroscience Research*, vol. 71, no. 1, pp. 121–126, 2003.

[60] F. Lao, L. Chen, W. Li et al., "Fullerene nanoparticles selectively enter oxidation-damaged cerebral microvessel endothelial cells and inhibit JNK-related apoptosis," *ACS Nano*, vol. 3, no. 11, pp. 3358–3368, 2009.

[61] J.-J. Yin, F. Lao, P. P. Fu et al., "The scavenging of reactive oxygen species and the potential for cell protection by functionalized fullerene materials," *Biomaterials*, vol. 30, no. 4, pp. 611–621, 2009.

[62] F. Caputo, M. De Nicola, and L. Ghibelli, "Pharmacological potential of bioactive engineered nanomaterials," *Biochemical Pharmacology*, vol. 92, no. 1, pp. 112–130, 2014.

[63] A. Djordjevic, J. M. Canadanovic-Brunet, M. Vojinovic-Miloradov, and G. Bogdanovic, "Antioxidant properties and hypothetic radical mechanism of fullerenol $C_{60}(OH)_{24}$," *Oxidation Communications*, vol. 27, no. 4, pp. 806–812, 2004.

[64] K. Kokubo, *Water-Soluble Single-Nano Carbon Particles: Fullerenol and Its Derivatives*, InTech, 2012.

[65] S. Kato, H. Aoshima, Y. Saitoh, and N. Miwa, "Highly hydroxylated or γ-cyclodextrin-bicapped water-soluble derivative of fullerene: the antioxidant ability assessed by electron spin resonance method and β-carotene bleaching assay," *Bioorganic and Medicinal Chemistry Letters*, vol. 19, no. 18, pp. 5293–5296, 2009.

[66] H. Ueno, S. Yamakura, R. S. Arastoo, T. Oshima, and K. Kokubo, "Systematic evaluation and mechanistic investigation of antioxidant activity of fullerenols using carotene bleaching assay-carotene bleaching assay," *Journal of Nanomaterials*, vol. 2014, Article ID 802596, 7 pages, 2014.

[67] K. D. Pickering and M. R. Wiesner, "Fullerol-sensitized production of reactive oxygen species in aqueous solution," *Environmental Science and Technology*, vol. 39, no. 5, pp. 1359–1365, 2005.

[68] B. Zhao, Y.-Y. He, C. F. Chignell, J.-J. Yin, U. Andley, and J. E. Roberts, "Difference in phototoxicity of cyclodextrin complexed fullerene [(γ-CyD)2/C_{60}] and its aggregated derivatives toward human lens epithelial cells," *Chemical Research in Toxicology*, vol. 22, no. 4, pp. 660–667, 2009.

[69] M. A. Orlova, T. P. Trofimova, A. P. Orlov, and O. A. Shatalov, "Perspectives of fullerene derivatives in PDT and radiotherapy of cancers," *British Journal of Medicine and Medical Research*, vol. 3, no. 4, pp. 1731–1756, 2013.

[70] B. Zhao, P. J. Bilski, Y.-Y. He, L. Feng, and C. F. Chignell, "Photo-induced reactive oxygen species generation by different water-soluble fullerenes (C_{60}) and their cytotoxicity in human keratinocytes," *Photochemistry and Photobiology*, vol. 84, no. 5, pp. 1215–1223, 2008.

[71] X.-J. Li, X.-H. Yang, L.-M. Song, H.-J. Ren, and T.-Z. Tao, "A DFT study on structure, stability, and optical property of fullerenols," *Structural Chemistry*, vol. 24, no. 4, pp. 1185–1192, 2013.

[72] Z. Wang, X. Chang, Z. Lu, M. Gu, Y. Zhao, and X. Gao, "A precision structural model for fullerenols," *Chemical Science*, vol. 5, no. 8, pp. 2940–2948, 2014.

[73] Z. Slanina, X. Zhao, L. Y. Chiang, and E. Osawa, "Biologically active fullerene derivatives: computations of structures, energetics, and vibrations of $C_{60}(OH)_x$ and $C_{60}(NO_2)_y$," *International Journal of Quantum Chemistry*, vol. 74, no. 3, pp. 343–349, 1999.

[74] J. G. Rodríguez-Zavala and R. A. Guirado-López, "Structure and energetics of polyhydroxylated carbon fullerenes," *Physical Review B*, vol. 69, no. 7, Article ID 075411, 13 pages, 2004.

[75] J. G. Rodríguez-Zavala and R. A. Guirado-López, "Stability of highly OH-covered C_{60} fullerenes: role of coadsorbed O impurities and of the charge state of the cage in the formation of carbon-opened structures," *The Journal of Physical Chemistry A*, vol. 110, no. 30, pp. 9459–9468, 2006.

[76] H. He, L. Zheng, P. Jin, and M. Yang, "The structural stability of polyhydroxylated $C_{60}(OH)_{24}$: density functional theory characterizations," *Computational and Theoretical Chemistry*, vol. 974, no. 1–3, pp. 16–20, 2011.